

INSTABILITY OF STATIONARY AND UNIFORMLY MOVING CYLINDRICAL FLUID BODIES—I

NEWTONIAN SYSTEMS

WEI-KUO LEE† and RAYMOND W. FLUMERFELT

Department of Chemical Engineering, University of Houston, Houston, TX 77004, U.S.A.

(Received 27 April 1980; in revised form 16 October 1980)

Abstract—The early work of Tomotika provides a basis for analyzing the instability of stationary and uniformly moving cylindrical fluid bodies. The classical results of Rayleigh, Christiansen and Weber for critical growth rates and wavenumbers are obtained as zero order limits of Tomotika's general solution expanded in terms of the key characteristic parameters: the viscosity ratio, the density ratio and the dispersed and continuous phase Ohnesorge numbers. By employing more than one characteristic time, these limits, as well as others, are obtained in a general solution framework. Numerical results provide insights into the effects of the physical forces, as well as criteria and bounds for the application of the limiting cases.

1. INTRODUCTION

A problem of long standing fundamental and practical importance in fluid mechanics is that of the instability and breakup of cylindrical fluid bodies. Since the early work of Plateau in 1873, such problems have occupied the interest of many investigators, and have played a key role in the development, analysis, and understanding of hydrodynamic stability and instability phenomena.

Practically, these problems are encountered in numerous industrial atomization, dispersion, and mixing operations. In some cases, drops are deformed by external flow fields into long cylindrical threads which subsequently break into smaller droplets. In others, liquid jets are injected into air or other liquids and disintegrate into small droplets. The creation of such dispersions may represent the final steps in the formation of a multiphase product, or may represent the intermediate steps in a transport or reaction process.

Early studies on the motion and instability of cylindrical fluid threads were mainly concerned with the disintegration of liquid jets. It is well known that during the formation of a jet in air, a wavy interface caused by external disturbances can amplify and finally result in the disintegration of the thread into a number of small droplets. If the motion is analyzed relative to a convected reference frame the problem is equivalent to that of a stationary liquid cylinder.

Theoretical interest in the instability of cylindrical fluid bodies originated with the early works of Plateau (1873) and Rayleigh (1878, 1879, 1892a, 1892b). Plateau correctly attributed the instability to the effect of surface tension. He concluded that a liquid cylinder under the influence of surface tension was unstable if its length was as long as its circumference. Rayleigh (1878) was the first to recognize that the jet was subject to disturbances at the nozzle of all possible wavelengths (or modes) and that the final critical wavelength corresponded to the mode with the largest growth rate. From potential energy considerations, Rayleigh developed relations for an inviscid liquid jet in an inviscid gas medium and showed that the most rapidly growing axisymmetric disturbance is the one for which $2\pi a/\lambda = 0.696$, where a is the initial radius of the jet and λ is the wavelength of the disturbance. Rayleigh's result was in agreement with the previous experimental observations of Savart which were reported by Plateau. Rayleigh (1879) also considered the effects of non-axisymmetric disturbance and found the liquid jet to be stable for all purely non-axisymmetric deformations. Somewhat later, he

†Present address: Exxon Research and Engineering Co., Linden, NJ 07036, U.S.A.

presented treatments of the instability of a viscous liquid jet in a gas (Rayleigh 1892a) and of a gas jet in an inviscid liquid (Rayleigh 1892b).

Tomotika (1935) obtained a relation which included the viscous and inertial effects of both phases, but limited his analysis and determination of the critical modes to systems with dominant viscous forces. Experimental support of Tomotika's analysis was given by the experimental results of Taylor (1934) on drop and thread breakup in shear and extensional flow fields. Christiansen (1955) and Christiansen & Hixson (1957) considered the case where the viscous effects in both the continuous and dispersed liquid phases were negligible. These results included as special cases the previous results of Rayleigh for systems with one phase being liquid and the other being a gas. More recently, Whitaker (1976) considered the effects of dynamic interfacial effects on the breakup of viscous liquid threads in an inviscid gas media.

Related studies have been reported by Ponstein (1959) who considered the instability of rotating cylindrical jets, and Goren (1961) who considered the instability of annular threads of fluid. All of these studies involved the use of linearized stability theory with the inherent assumption of small amplitude disturbances. Also, Goren (1964) used a variational approach involving minimum surface area and fixed volume to determine the shape of an unstable liquid thread.

Meister & Scheele (1967) have noted that the application of the limiting case analyses to jet and thread breakup problems under conditions which are consistent with the underlying theoretical assumptions has generally produced good agreement with experimental observations. However, the lack of clearly defined bounds of validity has often led to the application of these analyses in situations where they are not applicable. Obviously, incorrect interpretations and inaccurate predictions can then result. To avoid such difficulties and to identify the domain where each limiting relation is applicable, an appraisal of the problem, in full generality, is required. The work of Meister and Scheele was a step in this direction. Unfortunately, the limiting cases were identified in terms of physical statements rather than from limits of the characteristic dimensionless groups in the general solution. As a result, a clear and complete interpretation of the limiting cases was not obtained. In particular, the criteria established for the regions of validity of the limiting cases do not always encompass the complete domain of validity.

In the present work the problem of the instability of stationary cylindrical fluid bodies is analyzed and discussed from a unified viewpoint. A complete solution structure is presented in which the limiting cases are defined by restrictions on appropriate characteristic groups. This analysis clearly identifies the nature of the approximations and the relationship between Tomotika's results and the classical results of Rayleigh, Christiansen, and Weber, as well as other limiting cases not covered by these investigators.

2. BASIC EQUATIONS

Consider a stationary cylindrical column of a viscous fluid with its axis coincident with the z -axis in cylindrical coordinates (r, ϕ, z) immersed in an infinite mass of another viscous fluid. For incompressible Newtonian fluids with constant physical properties, if the axisymmetrical disturbance waves have amplitudes sufficiently small so that the non-linear inertial terms can be neglected, and if the body force effects are small compared to the viscous, inertial and interfacial effects, then the equation of motion for the disturbance velocity can be written as

$$\frac{\partial \mathbf{v}}{\partial t} = -\frac{1}{\rho} \nabla p + \nu \nabla^2 \mathbf{v} \quad [1]$$

where $\mathbf{v} = (u, v, w)$ and $\nu = \eta/\rho$ is the kinematic viscosity.

By introducing the Stokes stream function ψ and by eliminating pressure terms between the

component equations of motion, we obtain the linearized differential equation

$$\left(D - \frac{1}{\nu} \frac{\partial}{\partial t}\right) D\psi = 0, \tag{2}$$

where

$$D \equiv \left(\frac{\partial^2}{\partial r^2} - \frac{1}{r} \frac{\partial}{\partial r} + \frac{\partial^2}{\partial z^2}\right).$$

The above equation can be satisfied by motions proportional to the real part of $\exp(\alpha t + ikz)$. This gives the solution

$$\psi = \text{Re} \{ [C_1 r I_1(kr) + C_2 r K_1(kr) + C_3 r I_1(nr) + C_4 r K_1(nr)] \exp(\alpha t + ikz) \}$$

where

$$n \equiv \left(k^2 + \frac{\alpha}{\nu}\right)^{1/2}, \tag{3}$$

and α is the growth rate of the wave, k is the wave number, $I_q(x)$ and $K_q(x)$ are modified Bessel functions of order q with argument x , and C_1, C_2, C_3 and C_4 arbitrary constants to be determined by the boundary conditions.

The finiteness of the physical motions at $r=0$ and $r \rightarrow \infty$ gives the following stream functions:

$$\psi_D = \text{Re} \{ [C_{1D} r I_1(kr) + C_{3D} r I_1(lr)] \exp(\alpha t + ikz) \} \tag{4}$$

and

$$\psi_C = \text{Re} \{ [C_{2C} r K_1(kr) + C_{4C} r K_1(mr)] \exp(\alpha t + ikz) \} \tag{5}$$

where the subscripts D and C denote the dispersed and continuous phases respectively, and l and m are defined by

$$l \equiv \left(k^2 + \frac{\alpha}{\nu_D}\right)^{1/2} \text{ and } m \equiv \left(k^2 + \frac{\alpha}{\nu_C}\right)^{1/2}.$$

The boundary conditions at the interface of the two phases are:

- (1) The velocity is continuous at the interface,

$$[u_D = u_C]_{r=a}, \text{ and } [w_D = w_C]_{r=a}. \tag{6}$$

- (2) The shear stress is continuous at the interface,

$$[(P_{rz})_D = (P_{rz})_C]_{r=a} \text{ or } \left[\eta_D \left(\frac{\partial u_D}{\partial z} + \frac{\partial w_D}{\partial r} \right) = \eta_C \left(\frac{\partial u_C}{\partial z} + \frac{\partial w_C}{\partial r} \right) \right]_{r=a}. \tag{7}$$

- (3) The difference in the normal stress across the interface is due to the interfacial surface tension, or (with P as the total stress)

$$[(P_{rr})_C - (P_{rr})_D]_{r=a} = \Delta(P_{rr})_{r=a} = \Delta \left[-p + 2\eta \left(\frac{\partial u}{\partial r} \right) \right]_{r=a} = \sigma \left[\frac{1}{R_1} + \frac{1}{R_2} \right]_{r=a}. \tag{8}$$

Here Δ denotes the corresponding difference between the continuous and the dispersed phase quantities, and R_1 and R_2 are the principal radii of curvature of the interface. The integration of the z -component equation of motion will give the expression for the hydrostatic pressure p in terms of the velocity components, or alternatively the stream function ψ . Equation [8] can then be written as

$$\Delta \left\{ \frac{\eta}{k} \left[\frac{1}{r} \frac{\partial}{\partial r} \left(r \frac{\partial}{\partial r} \left(\frac{1}{r} \frac{\partial \psi}{\partial r} \right) - k^2 \psi \right) \right] - \frac{\alpha \rho}{kr} \left(\frac{\partial \psi}{\partial r} \right) - 2k\eta \frac{\partial}{\partial r} \left(\frac{\psi}{r} \right) \right\}_{r=a} = \left\{ \frac{\sigma k(1-k^2 a^2)}{\alpha a^3} \psi \right\}_{r=a}. \quad [9]$$

The constants in [4] and [5] are determined from the linear algebraic equations arising from the substitution of [4] and [5] into [6], [7] and [9]. Nontrivial solutions exist provided the determinant of the coefficient matrix of this system of linear homogeneous equations vanishes, and thus we obtain the frequency equation as:

$$\begin{vmatrix} I_1 & \bar{I}_1 & K_1 & \bar{K}_1 \\ XI_0 & X_D \bar{I}_0 & -XK_0 & -X_C \bar{K}_0 \\ 2UX^2 I_1 & U(X_D^2 + X^2) \bar{I}_1 & 2X^2 K_1 & (X_C^2 + X^2) \bar{K}_1 \\ F_1 & F_2 & F_3 & F_4 \end{vmatrix} = 0 \quad [10]$$

with

$$\begin{aligned} F_1 &= 2\pi_{1D}X(XI_0 - I_1) + \pi_{2D}I_0 + X(X^2 - 1)I_1, \\ F_2 &= 2\pi_{1D}X(X_D \bar{I}_0 - \bar{I}_1) + X(X^2 - 1)\bar{I}_1, \\ F_3 &= -[2\pi_{1C}X(XK_0 + K_1) + \pi_{2C}K_0], \\ F_4 &= -[2\pi_{1C}X(X_C \bar{K}_0 + \bar{K}_1)], \end{aligned}$$

where

$$\begin{aligned} X &= ka, \quad X_D = la, \quad X_C = ma, \quad U = \eta_D / \eta_C, \\ I_q &= I_q(X), \quad \bar{I}_q = I_q(X_D), \quad K_q = K_q(X), \quad \bar{K}_q = K_q(X_C), \\ \pi_{2D} &= \left(\frac{a^3 \alpha^2 \rho_D}{\sigma} \right), \quad \pi_{2C} = \left(\frac{a^3 \alpha^2 \rho_C}{\sigma} \right), \quad \pi_{1D} = \left(\frac{a \alpha \eta_D}{\sigma} \right) \end{aligned}$$

and

$$\pi_{1C} = \left(\frac{a \alpha \eta_C}{\sigma} \right).$$

Equation [10] was first derived by Tomotika (1935) and is the core relation in the instability problem of stationary cylindrical fluid bodies. Equation [10] gives a relation between the growth rate α , the wave length of the disturbance λ , and the geometry and physical properties of the fluid system. Since it is assumed that the cylindrical fluid thread is initially subjected to arbitrary disturbances involving all possible wavelengths, the critical wavelength λ^* at breakup corresponds to the mode with the largest growth rate α^* . The critical growth rate α^* indicates that rate at which the breakup process proceeds. For example, in jet breakup the larger the critical growth rate, the shorter the distance from the nozzle to the point of disintegration. The critical wavelength gives the distance between the breakup points along the thread, and therefore governs the ultimate drop size after breakup.

3. ANALYSIS

If we take a characteristic time θ and define the dimensionless growth rate as $S = \alpha\theta$, [10] can be written as

$$S^2 \left[\left(\frac{a^3 \rho_D}{\theta^2 \sigma} \right) \mathcal{F}_1 + \left(\frac{a^3 \rho_C}{\theta^2 \sigma} \right) \mathcal{F}_2 \right] + 2XS \left[\frac{a\eta_D}{\theta\sigma} - \frac{a\eta_C}{\theta\sigma} \right] \mathcal{F}_3 = X(X^2 - 1)\mathcal{F}_4 \tag{11}$$

where $\mathcal{F}_1, \mathcal{F}_2, \mathcal{F}_3$ and \mathcal{F}_4 are lengthy expressions involving modified Bessel functions and are listed in the Appendix.

For various characteristic times, the above equation can be expressed in terms of the following dimensionless quantities: the viscosity ratio $U(=\eta_D/\eta_C)$, the density ratio $G(=\rho_D/\rho_C)$, the Ohnesorge numbers defined as $Oh_D = (a\sigma\rho_D)^{1/2}/\eta_D$ and $Oh_C = (a\sigma\rho_C)^{1/2}/\eta_C$, the growth rate S , and the wave number X . (Here the Ohnesorge numbers are defined differently from the form $\eta/(a\sigma\rho)^{1/2}$ often used; see Ohnesorge 1936 and Miesse 1955.)

Note that the relation between the two Ohnesorge numbers is

$$G^{1/2} Oh_C = U Oh_D \tag{12}$$

For reasons to be discussed below, we pick characteristic times of the form $\theta_{I\beta} = (a^3 \rho_\beta / \sigma)^{1/2}$ and $\theta_{V\beta} = (a\eta_\beta / \sigma)$ where the first subscripts (I and V) refer to inertial and viscous effects, respectively, and the second subscript can be either D for dispersed phase or C for continuous phase. The corresponding dimensionless growth rate S for a given θ can then be defined as $S_{I\beta} = \alpha\theta_{I\beta}$ or $S_{V\beta} = \alpha\theta_{V\beta}$. In table 1 the forms of the dimensionless groups in [10] and [11] are listed for different selections of θ .

Terms in the last two rows of table 1 appear in the quantities $X_D^2 = [X^2 + (a^2\alpha/\nu_D)]$ and $X_C^2 = [X^2 + (a^2\alpha/\nu_C)]$. The dimensionless growth rates corresponding to the different characteristic times are related by

$$S_{ID} = G^{1/2} S_{IC} = Oh_D S_{VD} = Oh_D U S_{VC} \tag{13}$$

It is apparent from the results in table 1 and [12] that the problem can be expressed in terms of

Table 1. The characteristic times and the dimensionless parameters in the problem

$\pi \backslash \theta$	$\theta_{ID} = \left(\frac{a^3 \rho_D}{\sigma} \right)^{1/2}$	$\theta_{IC} = \left(\frac{a^3 \rho_C}{\sigma} \right)^{1/2}$	$\theta_{VD} = \left(\frac{a\eta_D}{\sigma} \right)$	$\theta_{VC} = \left(\frac{a\eta_C}{\sigma} \right)$
$\frac{a^3 \rho_D}{\theta^2 \sigma}$	1	G	Oh_D^2	$U^2 Oh_D^2$
$\frac{a^3 \rho_C}{\theta^2 \sigma}$	1/G	1	Oh_D^2/G	Oh_C^2
$\frac{a \eta_D}{\theta \sigma}$	1/ Oh_D	U/ Oh_C	1	U
$\frac{a \eta_C}{\theta \sigma}$	1/(U Oh_D)	1/ Oh_C	1/U	1
$\frac{a^2 \rho_D}{\theta \eta_D}$	Oh_D	$G^{1/2} Oh_D$	Oh_D^2	U Oh_D^2
$\frac{a^2 \rho_C}{\theta \eta_C}$	$Oh_C/G^{1/2}$	Oh_C	Oh_C^2/U	Oh_C^2

any three of the quantities U , G , Oh_D and Oh_C or any independent representation obtained therefrom, with S and X being the dependent variables.

Any one of the four characteristic times in table 1 can be used in Tomotika's general equation. However, for the limiting cases involving extreme values of Oh_D and Oh_C , we find that only specific characteristic times can be used to obtain meaningful results. In particular, in some cases where the Ohnesorge number approaches an extreme value, the dimensionless growth rate obtained from [10] or [11] can vanish even when the dimensional growth rate α is finite.

As an example, consider the case where $U = 1$ and $G = 1$ (note here $Oh_D = Oh_C$), and the characteristic time is $\theta_{VD} (= \theta_{VC}$ here). We see from figure 1(a) that S_{VD} vanishes as $Oh_D \rightarrow \infty$. However, the dimensional growth rate α is finite in this case as indicated by the results in figure 1(b) where a different characteristic time (θ_{ID}) is used. Clearly, in each case there is an appropriate characteristic time which provides a one-to-one correspondence between the dimensionless and dimensional growth rates. In the case just cited θ_{ID} is used for $Oh_D \rightarrow \infty$ and θ_{VD} for $Oh_D \rightarrow 0$.

Hence, to obtain meaningful limiting case results, more than one characteristic time is required. From the example just given, θ_{VB} is used for cases with small Ohnesorge numbers and θ_{IB} for large Ohnesorge numbers. Also, θ_{BD} is used for cases involving large values of U and G , i.e. when the dispersed phase effects dominate; θ_{BV} is used when U and G are small and continuous phase effects dominate.

Such comments are also appropriate with regard to the wavelength X . We see in figures 1(a) and 1(b) that the critical growth rate X^* varies from 0.5620 to 0.6769 as Oh_D takes on values from 0 to ∞ . Here again, the accurate determination of X^* at small Ohnesorge numbers requires the use of θ_{VD} (or θ_{VC}) and at large Ohnesorge numbers the use of θ_{ID} (or θ_{IC}).

4. LIMITING CASES

In this section a number of limiting cases of the problem are presented. The analysis starts from Tomotika's general relation,[10] or [11]. It is shown that the relations among the limiting cases can be clearly identified in terms of the Ohnesorge numbers, the viscosity ratio, and the density ratio. A summary of all these relations is given in figure 2. The limiting cases in the upper portion of this figure are those where viscous effects dominate; the upper right corner

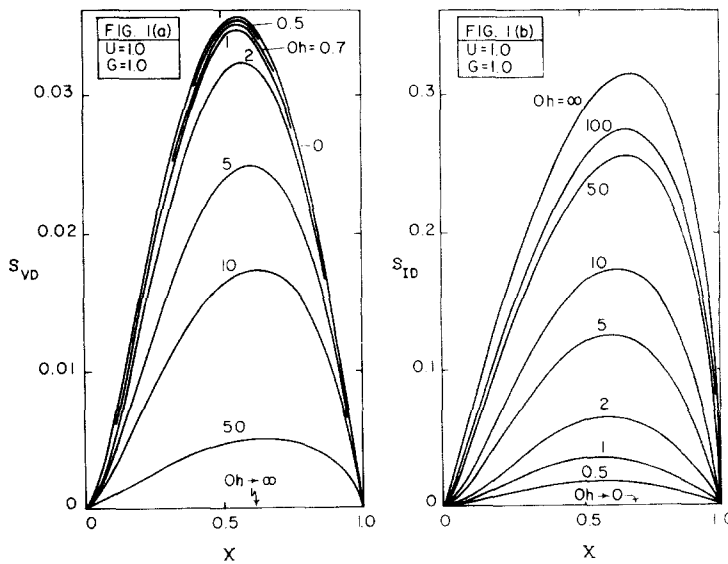


Figure 1. Growth rates and wavenumbers for systems with equal viscosities and densities. (Note here, $Oh = Oh_D = Oh_C$ as $U = G = 1$.)

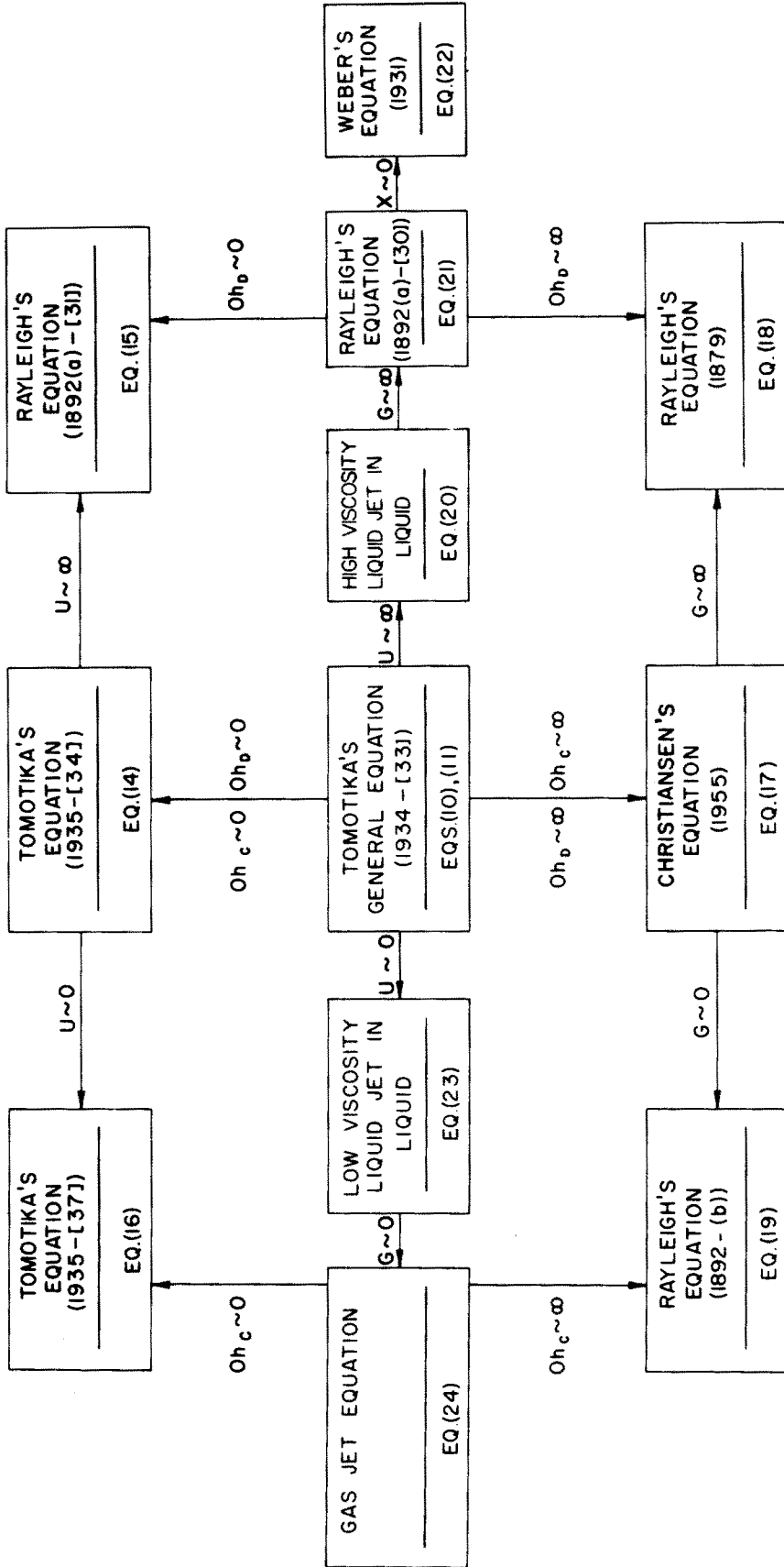


Figure 2. Summary of equations for the hydrodynamic instability of stationary and uniformly moving cylindrical fluid bodies ($U = \eta \rho / \eta_c$, $G = \rho g / \rho_c$, $Oh_D = (\sigma \rho g)^{1/2} / \eta_D$, $Oh_C = (\sigma \rho c)^{1/2} / \eta_C$, and $X = 2\pi d / \lambda$).

corresponds to dominant dispersed phase viscous effects and the left corner to dominate continuous phase viscous effects. The inertial effects are dominant in the lower portion of the figure, with the right corner corresponding to dispersed phase dominance and the left corner to continuous phase dominance. We now summarize the growth rate–wavelength expressions for the limiting cases shown in figure 2.

(a) $Oh_D \sim 0$, $Oh_C \sim 0$

In this case we obtain Tomotika's special equation (Tomotika 1935, [34]) which can be deduced from [11] by a Taylor expansion about the indicated limiting values of the characteristic groups. Tomotika obtained this equation from an expansion about $\rho_D \sim 0$, $\rho_C \sim 0$, however, its applicability is much broader than this, as the dimensionless form of the limit indicates. The equation for this limit can be represented by:

$$\begin{vmatrix} I_1 & XI_0 - I_1 & K_1 & -XK_0 - K_1 \\ I_0 & I_0 + XI_1 & -K_0 & XK_1 - K_0 \\ UI_1 & UXI_0 & K_1 & -XK_0 \\ M_1 & M_2 & M_3 & M_4 \end{vmatrix} = 0 \quad [14]$$

where

$$M_1 = UI_1' S + \frac{(X^2 - 1)I_1}{\left(\frac{a\eta_C}{\theta\sigma}\right)2X}$$

$$M_2 = U(I_1' + XI_1'' - I_0)S + \frac{(X^2 - 1)I_1'}{2\left(\frac{a\eta_C}{\theta\sigma}\right)}$$

$$M_3 = K_1' S$$

and

$$M_4 = (K_1' + XK_1'' + K_0)S.$$

Here, the characteristic times containing viscosities are used. As explained previously, we will use θ_{VD} for the cases $U \geq 1$, and θ_{VC} for the cases $U \leq 1$. The subcases in this category are:

(i) $U \rightarrow \infty$. In the case where the viscosity-ratio becomes larger and larger, [14] gives the growth rate (with θ_{VD} used as a characteristic time) as

$$S_{VD} = \left[\frac{(X^2 - 1)/2}{1 + X^2 - (XI_0/I_1)^2} \right] \quad [15]$$

which agrees with the equation derived by Rayleigh (1892(a), [31]) for a low density viscous jet in a "vacuum" (low density, inviscid) medium.

(ii) $U \rightarrow 0$. As $U \rightarrow 0$, [14] reduces to the form,

$$S_{VC} = \left[\frac{(1 - X^2)/2}{1 + X^2 - (XK_0/K_1)^2} \right] \quad [16]$$

which is the same as a relation given by Tomotika (1935, [37]) for the system of a "vacuum" jet in a low density viscous medium.

(b) $Oh_D \sim \infty$; $Oh_C \sim \infty$

By these limits, we can derive Christiansen's equation (1955) from [11] as:

$$S_{ID}^2 = \frac{X(1 - X^2)}{(I_0/I_1) + (K_0/K_1)/G} \quad [17a]$$

or

$$S_{IC}^2 = \frac{X(1-X^2)}{G(I_0/I_1) + (K_0/K_1)} \tag{17b}$$

These equations can be reduced further to the cases corresponding to large and small G .

(i) $G \rightarrow \infty$. In this case, [17a] reduces to

$$S_{ID}^2 = X(1-X^2)(I_1/I_0) \tag{18}$$

which is the famous relation given by Rayleigh (1879) for an inviscid jet in a vacuum medium. Although it was derived here from [17a], there is actually no constraint on Oh_c since it can also be derived from another equation obtained by Rayleigh (1892a, [30]) with $U \rightarrow \infty$, $G \rightarrow \infty$ and $Oh_D \rightarrow \infty$ (see figure 2).

(ii) $G \rightarrow 0$. With $Oh_c \sim \infty$ and $G \sim 0$, [17b] reduces to

$$S_{IC}^2 = X(1-X^2)(K_1/K_0) \tag{19}$$

which is identical to another relation derived by Rayleigh (1892b) for a vacuum jet in an inviscid medium. It can be seen that only Oh_c is required to be defined here, and Oh_D is not a key parameter in this case.

(c) $U \sim \infty$

If we have $U \gg 1$ and the other parameters kept finite, [11] can be reduced to

$$S_{ID}^2 f_1 + 2XS_{ID} f_2 / Oh_D = X(1-X^2) f_3 + f_4 \tag{20a}$$

or

$$Oh_D^2 S_{VD}^2 f_1 + 2XS_{VD} f_2 = X(1-X^2) f_3 + f_4 \tag{20b}$$

with

$$f_1 = \frac{I_0}{I_1} \left[1 + \frac{1}{G} \left(\frac{X_D \bar{I}_0 / \bar{I}_1 + XK_0 / K_1}{X_C \bar{K}_0 / \bar{K}_1 - XK_0 / K_1} \right) \right] + \frac{K_0}{GK_1} \left[\left(\frac{X_C \bar{K}_0 / \bar{K}_1 + XI_0 / I_1}{X_C \bar{K}_0 / \bar{K}_1 - XK_0 / K_1} \right) + \frac{1}{G} \left(\frac{X_D \bar{I}_0 / \bar{I}_1 - XI_0 / I_1}{X_C \bar{K}_0 / \bar{K}_1 - XK_0 / K_1} \right) \right],$$

$$f_2 = \left(2X \frac{I_0}{I_1} - 1 \right) - \frac{1}{G} \left[\left(2X \frac{K_0}{K_1} + 1 \right) \cdot \left(\frac{X_D \bar{I}_0 / \bar{I}_1 - XI_0 / I_1}{X_C \bar{K}_0 / \bar{K}_1 - XK_0 / K_1} \right) \right],$$

$$f_3 = \left(1 + \frac{1}{G} \left(\frac{X_D \bar{I}_0 / \bar{I}_1 - XI_0 / I_1}{X_C \bar{K}_0 / \bar{K}_1 - XK_0 / K_1} \right) \right),$$

and

$$f_4 = \left[X_D \frac{\bar{I}_0}{\bar{I}_1} - X \frac{I_0}{I_1} \right] \cdot \frac{4X^3}{Oh_D^2}.$$

Equivalent forms with θ_r selected as the characteristic time can also be written by referring to [13]. Yet those are mainly used for systems with small G , and these less practical systems (with $U \sim \infty$ and $G \sim 0$) are not considered here.

Equation [20a] and [20b] can be used in cases where a highly viscous liquid jet or thread breaks up in a low viscosity liquid medium.

(i) $U \sim \infty$, $G \sim \infty$. For large density ratios and finite Oh_D , [20a] and [20b] reduce to

$$\frac{I_0}{I_1} S_{ID}^2 + \frac{2X}{Oh_D} S_{ID} \left(2X \frac{I_0}{I_1} - 1 \right) = X(1 - X^2) + \frac{4X^3}{Oh_D^2} \left(X_D \frac{\bar{I}_0}{\bar{I}_1} - X \frac{I_0}{I_1} \right) \quad [21a]$$

or

$$\frac{I_0}{I_1} Oh_D^2 S_{VD}^2 + 2XS_{VD} \left(2X \frac{I_0}{I_1} - 1 \right) = X(1 - X^2) + \frac{4X^3}{Oh_D^2} \left(X_D \frac{\bar{I}_0}{\bar{I}_1} - X \frac{I_0}{I_1} \right) \quad [21b]$$

which are the same as the equations derived by Rayleigh (1892a, [30]). This equation is applicable to those cases involving a highly viscous liquid jet moving in a gas medium.

In those cases where $Oh_D \rightarrow 0$, we can obtain [15] from [21b] by expanding it around $Oh_D^2 \sim 0$ (see Lee 1972 for details). For the cases where $Oh_D \rightarrow \infty$, [21a] will give [18]—another relation derived by Rayleigh.

Normally, unstable wave motions occur when $X < 1$, and by taking the limit as $X \rightarrow 0$, [21] reduces to the equation of Weber (1931):

$$S_{ID}^2 + \frac{3X^2}{Oh_D} S_{ID} = \frac{X^2(1 - X^2)}{2} = Oh_D^2 S_{VD}^2 + 3X^2 S_{VD}. \quad [22]$$

This equation has been widely used and is shown here as a special case of Rayleigh's equation ([21a] or [21b] here) with a term $(2X^2/Oh_D) \cdot (\partial S/\partial X)_{X \rightarrow 0}$ on the r.h.s. of [21a] or [21b] neglected (see Lee 1972). This equation can be used for all values of Oh_D , and apparently can also be reduced to the simplified forms of [15] and [18] with Oh_D approaching zero and infinity, respectively.

(d) $U \sim 0$

With finite values of the Ohnesorge numbers and the density ratio, [11] can be reduced to the following form for very small values of U :

$$S_{IC}^2 g_1 + \frac{2XS_{IC}}{Oh_C} g_2 = X(1 - X^2)g_3 + g_4 \quad [23a]$$

or

$$Oh_C^2 S_{VC}^2 g_1 + 2XS_{VC} g_2 = X(1 - X^2)g_3 + g_4 \quad [23b]$$

with

$$g_1 = \frac{GI_0}{I_1} \left[G \left(\frac{X_C \bar{K}_0 / \bar{K}_1 - XK_0 / K_1}{X_D \bar{I}_0 / \bar{I}_1 - XI_0 / I_1} \right) - \left(\frac{X_D \bar{I}_0 / \bar{I}_1 + XK_0 / K_1}{X_D \bar{I}_0 / \bar{I}_1 - XI_0 / I_1} \right) \right] + \frac{K_0}{K_1} \left[G \left(\frac{X_C \bar{K}_0 / \bar{K}_1 + XI_0 / I_1}{X_D \bar{I}_0 / \bar{I}_1 - XI_0 / I_1} \right) + 1 \right],$$

$$g_2 = \left[G \left(1 - 2X \frac{I_0}{I_1} \right) \cdot \left(\frac{X_C \bar{K}_0 / \bar{K}_1 - XK_0 / K_1}{X_D \bar{I}_0 / \bar{I}_1 - XI_0 / I_1} \right) + 2X \frac{K_0}{K_1} + 1 \right],$$

$$g_3 = \left[G \left(\frac{X_C \bar{K}_0 / \bar{K}_1 - XK_0 / K_1}{X_D \bar{I}_0 / \bar{I}_1 - XI_0 / I_1} \right) + 1 \right],$$

and

$$g_4 = \frac{4X^3}{Oh_C^2} \left(X_C \frac{\bar{K}_0}{\bar{K}_1} - X \frac{K_0}{K_1} \right).$$

This relation can be used for a low viscosity liquid thread in liquid medium.

An important sub-case in this category is the limiting case where a gas jet is injected into some low viscosity liquid medium with $G \sim 0$ while Oh_C is still finite. This gives

$$\frac{K_0}{K_1} S_{IC}^2 + \frac{2X}{Oh_C} \left[2X \frac{K_0}{K_1} + 1 \right] S_{IC} = X(1 - X^2) + g_4 \tag{24a}$$

or

$$\frac{K_0}{K_1} Oh_C^2 S_{VC}^2 + 2X \left[2X \frac{K_0}{K_1} + 1 \right] S_{VC} = X(1 - X^2) + g_4. \tag{24b}$$

Further simplification can be made to reduce [24a] to [19] as $Oh_C \rightarrow \infty$ and [24b] to [16] as $Oh_C \rightarrow 0$. In the latter case, we need to expand [24b] around $Oh_C^2 = 0$ (see Lee 1972).

It should be noted that equivalent forms of the above equations can also be written with $\theta_{\beta D}$ instead of $\theta_{\beta C}$. Yet those equations are only interesting in the cases where $U \sim 0$ and $G \sim \infty$, which are not often realized in practice, and therefore, are not presented here.

5. NUMERICAL RESULTS

Some numerical computations are now presented to confirm the above analysis and to provide a basis for determining the range over which the limiting cases are valid. In these computations, the physical properties of the dispersed phase are used when $U \geq 1$, and those of the continuous phase when $U \leq 1$. As for the characteristic times, those containing the inertial effects, $\theta_{I\beta}$, are used in the systems with large Ohnesorge numbers and those containing the viscous effects, $\theta_{V\beta}$, are used in the systems with small Ohnesorge numbers. In addition to showing the ranges of validity of the limiting case solutions more clearly, these selections of the characteristic times also provide higher computational stability.

All of the results are obtained as unstable motions for the range $X < 1$ with the shape of curves shown in figure 1(a, b). Since the motions are exponentially proportional to $(\alpha t + ikz)$, only the mode with maximum growth rate will be shown and discussed in the following illustrations.

In figure 3, the maximum growth rates and their corresponding values of wavenumber, X^* , are shown for the systems with $G = 1$ and $U \geq 1$. The characteristic times θ_{ID} and θ_{VD} are used for the cases with high (figure 3a) and low (figure 3b) values of Oh_D , respectively. In figure 3(a, b) the point P corresponds to the case where $U \sim \infty$ and $Oh_D \sim 0$, which is the case given by [15]. The point Q , with $Oh_D \sim \infty$ for all U , is the result given either by [17a] or [17b], which are alternative forms of Christiansen's equation. It can be seen that the problem converges to the extreme cases rapidly in both of the parameters Oh_D and U . The point R denotes systems with $Oh_D \sim 0$ and $U = 1$, a case which is seldom encountered in actual practice.

Since

$$\alpha^* = (\sigma/a^3 \rho_D)^{1/2} S_{ID}^*,$$

we note from figure 3(a) that for systems with equal dispersed phase and continuous phase densities, an increase in the continuous phase viscous effects (or forces) relative to the other physical effects (inertial and interfacial) produces lower values of α^* and higher values of X^* , which physically results in longer breakup lengths in jets and smaller drops after breakup. Increases in the interfacial forces result in shorter breakup lengths and smaller drops. Also, noting that

$$\alpha^* = (\sigma/a\eta_D) S_{VD}^*,$$

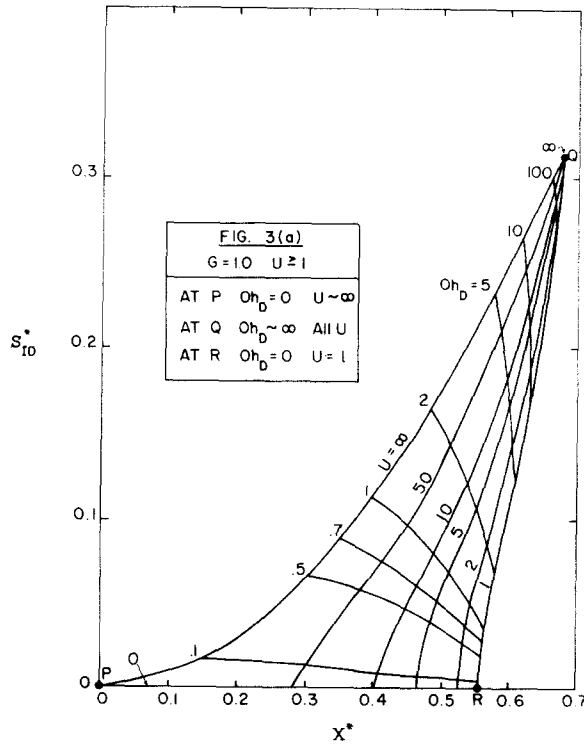


Figure 3(a). Critical growth rate and wavenumber results— $G = 1.0$, $U \geq 1$; large Oh_D results. At point P , $Oh_D = 0$, $U \sim \infty$; at point Q , $Oh_D \sim \infty$ for all U ; at point R , $Oh_D = 0$, $U = 1$. (Note that the results with $Oh_D = 0$ coincide with the ordinate.)

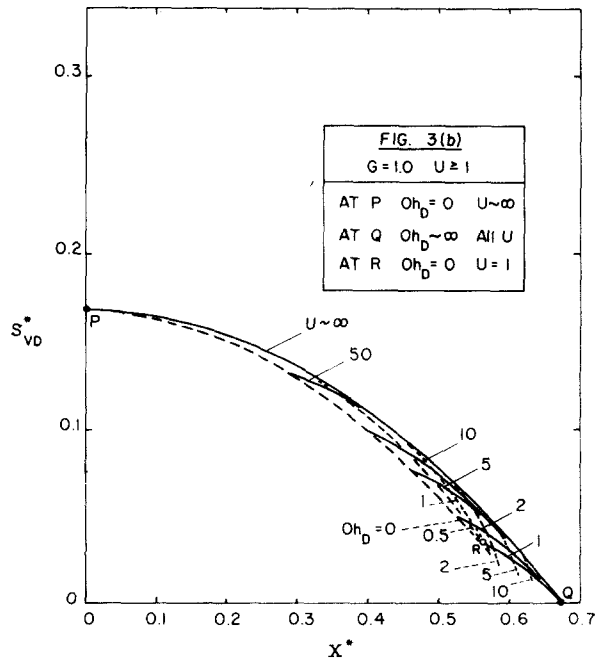


Figure 3(b). Critical growth rate and wavelength results— $G = 1.0$, $U \geq 1$; Small Oh_D results. Points P , Q and R are the same limits indicated in figure 3(a). (Note, in this case, the results with $Oh_D = 0$ show finite critical growth rate.)

we see from figure 3(b) that an increase in the inertial forces (or an increase in both ρ_D and ρ_C with $G = 1$) produces longer breakup lengths and smaller drops. Finally, both figures 3(a) and 3(b) indicate that the largest drops result from systems with high viscosity ratios and systems with small values of Oh_D .

For systems with $G = 1$ and $U \leq 1$, similar figures for S^* and X^* can also be obtained with θ_{VC} and θ_{VC} as characteristic times. We show here only the results for the critical wavenumbers X^* together with the results for $U \geq 1$ in figure 4.

The parameters used in figure 4 are Oh_C and Oh_D for the systems $U < 1$ and $U > 1$, respectively. The two sets of curves match one another at $U = 1$ in this example since $G = 1$. The top curve is a horizontal line through $X^* = 0.6769$ which corresponds to the result from Christiansen's equation when $Oh_D \sim Oh_C \sim \infty$. The bottom curve is that corresponding to Tomotika's equation (1935, [34]) with $Oh_D \sim Oh_C \sim 0$. Curves between these two limiting cases are those with intermediate Ohnesorge number values. It can be seen that X^* is particularly sensitive to changes in Oh_D (or Oh_C) at the lower values of these parameters. The two ends of these curves approach the limiting cases of $U \rightarrow 0$ and $U \rightarrow \infty$, which correspond to the results from [23] and [20], respectively. Two dashed curves starting at about $U = 0.28$ and $Oh_C = 0$ show the loci of the X^* maxima as a function of Ohnesorge numbers. Since the points on these loci give the minimum size of droplets resulting from the breakup of the cylindrical fluid body, these results support the common observation in mixing processes that the best dispersion (smallest drops) can be obtained with fluids of similar viscosities. The results here show that this is generally true for systems of small and moderate Ohnesorge numbers.

In figure 5(a, b) we show results for $U \sim \infty$, the first being for the smaller Oh_D values and the second for the larger values. Point P denotes the solution of Rayleigh's equation ([15]) with $Oh_D = 0$. The curve QR denotes Christiansen's equation ([17]) with $Oh_D \sim \infty$, and the points Q and R are results from [18] and [19] with $G \sim \infty$ and 0 respectively. It can be seen that the motions with $Oh_D = 1$ are again in the middle between the extreme ends $Oh_D = 0$ and $Oh_D \sim \infty$ and the convergence is fast toward each end. The changes due to density ratios from 0 to 1 are much larger than those from 1 to ∞ and, in fact, the cases $G \geq 1$ can be replaced by the extreme end with $G \sim \infty$ without much error. It should be pointed out that the situations around point Q ($U \rightarrow \infty$ and $G \rightarrow 0$) are seldom realized with real systems. Also, the numerical computations become somewhat unstable in these cases. The dimensionless growth rates S_{ID} and S_{VD} vanish in these computations, yet as mentioned previously, this does not mean the motions are stable. Since these problems are of little practical interest, we do not discuss these in detail here.

Physically, the results in figure 5(a, b) infer that for systems with $U \sim \infty$, increases in

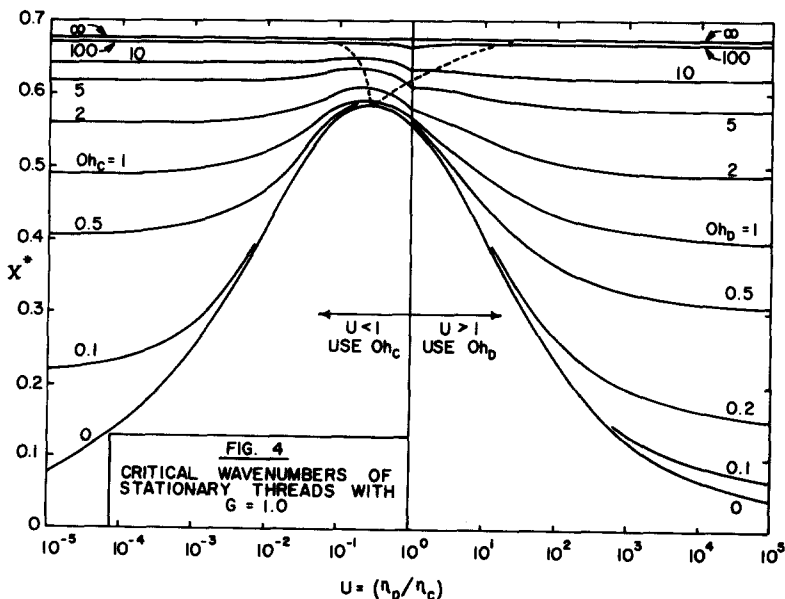


Figure 4. Critical wavenumbers of stationary threads with $G = 1.0$.

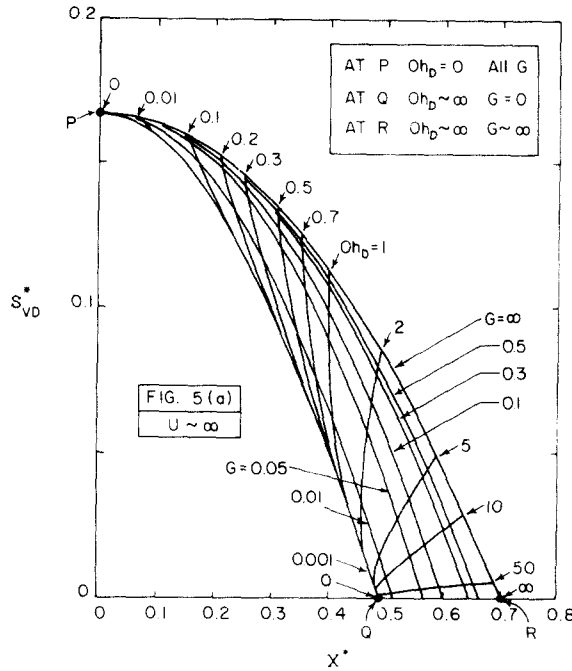


Figure 5(a). Critical growth rates and wavenumbers for systems with $U \sim \infty$ and small Oh_D . At point P , $Oh_D = 0$, for all G ; at point Q , $Oh_D \sim \infty$, $G = 0$; at point R , $Oh_D \sim \infty$, $G \sim \infty$.

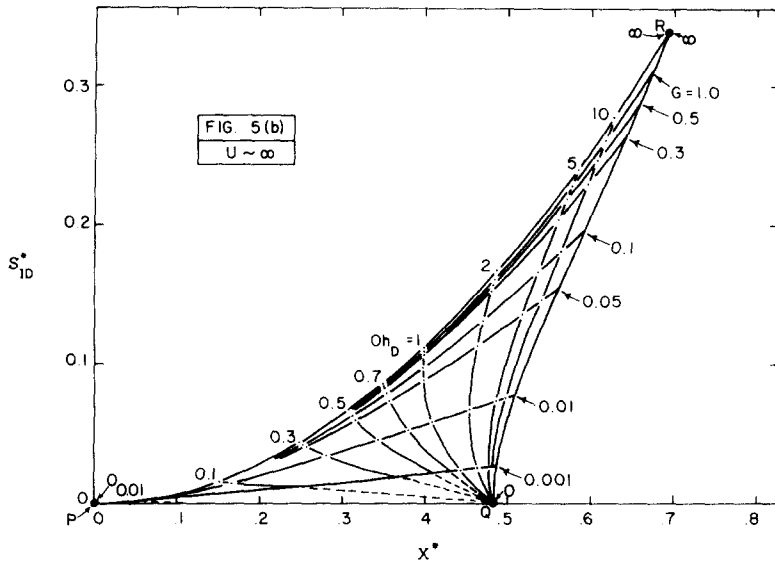


Figure 5(b). Critical growth rates and wavenumbers for systems with $U \sim \infty$ and large Oh_D . Points P , Q and R are the same limits indicated in figure 5(a).

continuous phase inertial forces or dispersed phase viscous forces result in longer jet breakup lengths. Also, by the values of X^* , we conclude that larger droplets are formed in systems with $Oh_D > 2$ in the former case and smaller drops in systems with $Oh_D < 1$. Increases in dispersed phase inertial forces also result in longer jet breakup lengths and smaller drops. Finally, shorter jets and smaller droplets are produced with increases in the interfacial forces—the same observation as noted for the $G = 1$ case represented in figures 3 and 4.

As for the limiting cases with $U = 0$, the results are shown in figure 6(a, b) with Oh_C and G as parameters. The basic features are similar to those in the case of $U \rightarrow \infty$. Point P denotes the result of Tomotika's equation ([16]) with $Oh_C = 0$, and curve QR shows the result of Christian-

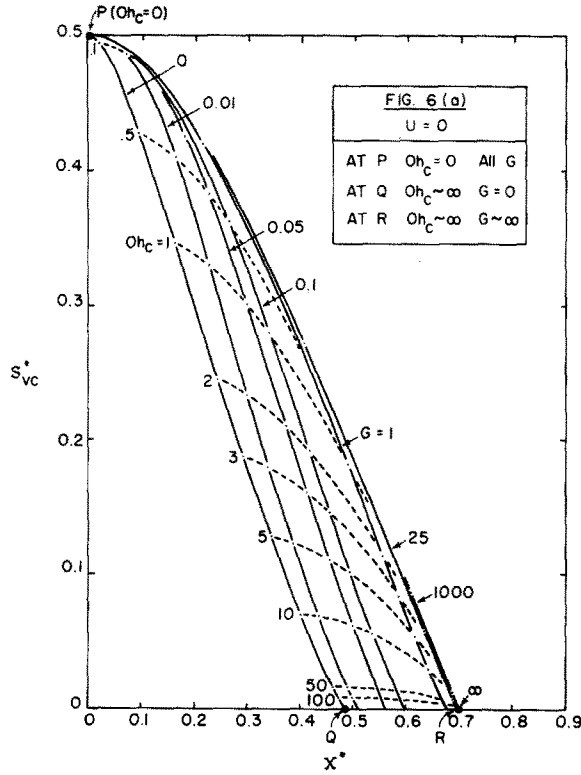


Figure 6(a). Critical growth rates and wavenumbers for systems with $U = 0$; small Oh_C results. At point P , $Oh_C \sim 0$ (all G); at point Q , $Oh_C \sim \infty$, $G = 0$; at point R , $Oh_C \sim \infty$, $G \sim \infty$.

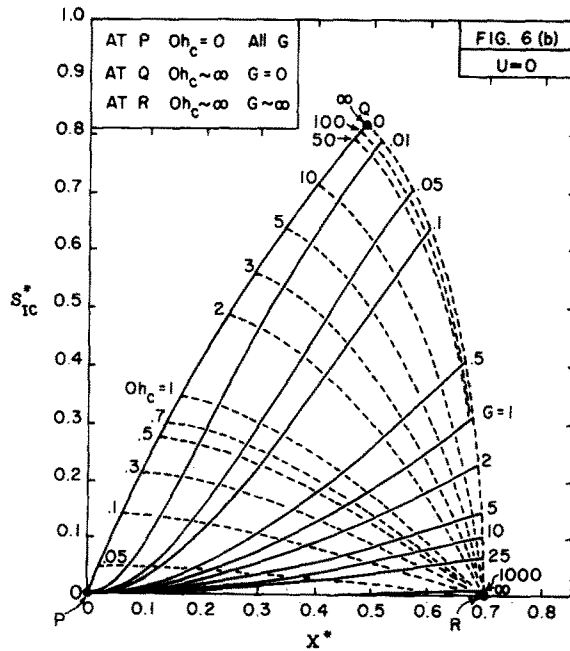


Figure 6(b). Critical growth rates and wavenumbers for systems with $U = 0$; large Oh_C results. Points P , Q and R are the same limits indicated in figure 6(a).

sen's equation ([17]). Point R denotes another physical situation seldom encountered in practice ($Oh_C \rightarrow \infty$, $U = 0$).

The results in figure 6(a, b) for systems with $U = 0$ indicate that shorter breakup lengths and smaller dispersion droplets are produced when the continuous phase viscous effects are

decreased and the interfacial effects are increased. The dispersed phase inertial effects, when increased, produce longer breakup lengths and smaller droplets.

It is also interesting to show the results for the limiting case given by Tomotika (1935, [34]; [14] in this paper). These results are shown in figure 7. Note here that critical growth rate-wavelength results are represented by the dotted line corresponding to the maximum value of α at each value of U . Physically, these results would arise in systems where the viscous effects tend to dominate. When $U = 0$, we obtain the limit given by Tomotika ([16]) and when $U \rightarrow \infty$ we obtain one of Rayleigh's relations ([15]). These results infer longer jet breakup lengths with increasing continuous phase or dispersed phase viscosity. Also, the minimum size drops are produced when $U = 0.28$, a result already cited in connection with figure 4.

6. REGIONS OF APPLICABILITY—LIMITING CASES

The limiting solutions of Tomotika's general equation can often be used to predict the growth rate and the wavelength in many situations of practical interest. The principal concern in these cases is the degree to which a given limiting solution is applicable. As yet, quantitative criteria for determining whether a limiting solution is applicable have not been clearly established. As noted previously, Meister & Scheele (1967) were concerned with this problem and presented criteria for a number of physical situations, however, their criteria were somewhat narrow and did not encompass the full range of possible physical situations which could arise.

In the work here we have obtained bounds of validity for the four limiting cases occupying the corners in figure 2; specifically, [15], [16], [18] and [19]. Each of these limits were interpreted as the zero order term in a Taylor series expansion of S^* or X^* in terms of the appropriate characteristic dimensionless groups. For instance, in the case of Rayleigh's equation (1892b; [19] of this paper) the characteristic groups are G , $1/Oh_c$, and $1/(G^{1/2}Oh_D)$ and the expansion is about the point $(0, 0, 0)$. For the dimensionless growth rate we obtain

$$S_{IC}^* = S_{IC}^*(0, 0, 0) + \left(\frac{\partial S_{IC}^*}{\partial G}\right)_0 G + \left(\frac{\partial S_{IC}^*}{\partial(1/Oh_c)}\right)_0 (1/Oh_c) + \left(\frac{\partial S_{IC}^*}{\partial(1/G^{1/2}Oh_D)}\right)_0 (1/(G^{1/2}Oh_D))$$

+ second and higher order terms.

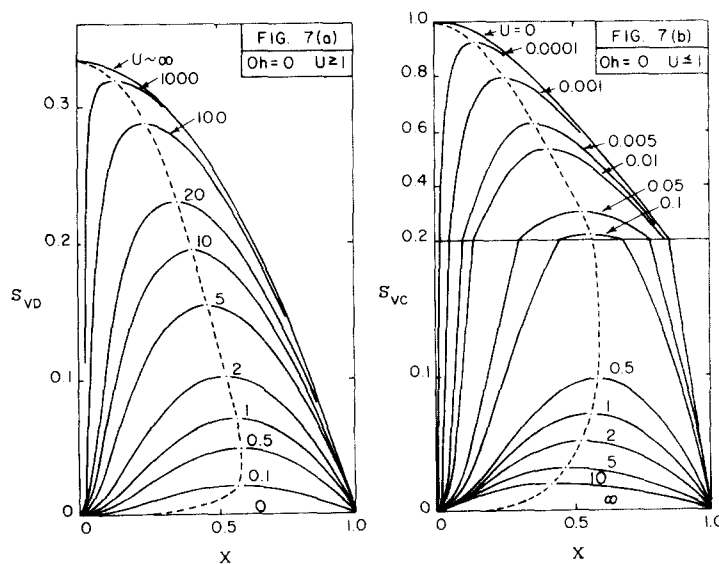


Figure 7. Growth rates and wavenumbers for systems with vanishing Ohnesorge numbers. Dotted line refers to critical growth rate—wavenumber relation.

The region of validity of the limit $S_{IC}^*(0, 0, 0)$ corresponding to some acceptable error level ϵ is then

$$k_1(G) + k_2(1/Oh_C) + k_3(1/(G^{1/2} Oh_D)) < \epsilon$$

where k_1 is the magnitude of the maximum value of $(\partial S_{IC}^*/\partial G)$ over the interval in question, i.e. from $(0, 0, 0)$ to $(G, 1/Oh_C, (1/(G^{1/2} Oh_D)))$; k_2 and k_3 being similar derivatives with respect to $1/Oh_C$ and $(1/(G^{1/2} Oh_D))$, respectively.

In the work here the coefficients k_1 , k_2 and k_3 were estimated from numerical calculations in the vicinity of the limit point using Tomotika's general equation. In each case, conservative estimates were used in establishing the bounds of validity. The details of these calculations are described elsewhere (Yu 1974). We list here only the results corresponding to a 5 per cent error bound.

(a) *Rayleigh's equation* (1892 b, [19] of this paper)

This limit arises when $Oh_C \rightarrow \infty$, $(G^{1/2} Oh_D) \rightarrow \infty$ and $G \rightarrow 0$ (implicit: $U \rightarrow 0$). The critical growth rate and wavelength values for this limit are

$$\alpha^* = 0.819(\sigma/a^3 \rho_C)^{1/2} \tag{25}$$

$$\lambda^* = 12.96a. \tag{26}$$

For 5 per cent error (or less) in S^* and X^* , the following criteria define the regions of validity:

$$S_{IC}^*: 74.4G + \frac{30.0}{Oh_C} + \frac{7.3}{G^{1/2} Oh_D} < 1 \tag{27}$$

$$X^*: 1120G + \frac{44.8}{Oh_C} + \frac{10.3}{G^{1/2} Oh_D} < 1. \tag{28}$$

Meister and Schelle obtained the criteria for a maximum 5 per cent error in the growth rate to be

$$Oh_C > 25.5.$$

Obviously, from [27] and [28] this criteria would be valid only for sufficiently small values of G and $(G^{1/2} Oh_D)^{-1}$. Since G must be quite small and Oh_C must be quite large to satisfy [27] and [28], this limit is often referred to as a gas jet in a low viscosity liquid.

(b) *Rayleigh's equation* (1879, [18] of this paper)

This limit is realized when $Oh_D \rightarrow \infty$, $Oh_C^2/G \rightarrow \infty$, and $G \rightarrow \infty$ (implicit: $U \rightarrow \infty$). Physically, this limit might be thought of as a low-viscosity liquid in a gas. The critical growth rate and wavenumbers are

$$\alpha^* = 0.344(\sigma/a^3 \rho_D)^{1/2} \tag{29}$$

$$\lambda^* = 9.03a \tag{30}$$

and the regions of validity (to 5 per cent maximum error) are defined by

$$S_{ID}^*: \frac{38.8}{Oh_D} + \frac{4.08}{G} + 1.54 \left(\frac{G^{1/2}}{Oh_C} \right) < 1 \tag{31}$$

$$X^*: \frac{20.3}{Oh_D} + \frac{0.86}{G} + 0.12 \left(\frac{G^{1/2}}{Oh_C} \right) < 1. \tag{32}$$

The criterion given by Meister and Scheele for 5 per cent maximum error in the growth rate is

$$\text{Oh}_D > 14.2 .$$

Here again, their criterion does not seem to be sufficiently general. Also, no criterion is given for the wavelength λ^* .

(c) *Tomotika's equation* (1935, [37]; [16] in this paper)

This limit is defined by $U \rightarrow 0$, $\text{Oh}_C \rightarrow 0$, and $U \text{Oh}_D^2 \rightarrow 0$ ($G \rightarrow 0$, implicit). The critical growth rate and wavelength are

$$\alpha^* = 0.5\sigma/a\eta_C \quad [33]$$

$$\lambda^* \rightarrow \infty . \quad [34]$$

For 5 per cent maximum error in S_{VD}^* we have

$$14,000U + 8.00\text{Oh}_C^2 + 0.08U \text{Oh}_D^2 < 1 . \quad [35]$$

No meaningful bound on λ^* is possible in this case. Physically, this case might correspond to a gas jet in a highly viscous liquid.

(d) *Rayleigh's equation* (1892a, [37]; [15] this paper)

This limit is defined by $\text{Oh}_D \rightarrow 0$, $\text{Oh}_C^2/U \rightarrow 0$, and $U \rightarrow \infty$ ($G \rightarrow \infty$, implicit). The critical growth rate and wavelength are

$$\alpha^* = 0.166\sigma a/\eta_D \quad [36]$$

$$\lambda^* \rightarrow \infty . \quad [37]$$

The limit for α^* is valid to 5 per cent within the region

$$S_{VD}: \frac{903}{U} + 84.3 \text{Oh}_D^2 + 0.42 \frac{\text{Oh}_C^2}{U} < 1 . \quad [38]$$

This case might correspond to a highly viscous liquid jet in a gas. Meister and Scheele obtained

$$\text{Oh}_D < 0.85$$

as a 5 per cent criterion on α^* in this case.

7. CONCLUDING REMARKS

It is clear from the results of the previous sections that the breakup of cylindrical fluid bodies involves a complex interaction between interfacial, viscous, and inertial forces. The characteristic groups which naturally arise in these problems are the viscosity ratio, the density ratio, and the continuous and dispersed phase Ohnesorge numbers. In order to present the problem in a unified dimensionless framework with all of the classical results and their limiting domains identified, it is necessary to employ more than one characteristic time. Quantitatively, the limiting relations appear to have a large range of applicability, and hence it is not surprising that they have been used extensively in the past with considerable success.

A new relation ([23]) is obtained for the cases where $U \sim 0$. This equation, together with its subsequent limiting forms, should be useful in situations where low viscosity liquid threads

breakup in highly viscous surroundings. Such situations can arise in dispersion and mixing operations encountered in the polymer process industry.

Finally, we note that the present analysis is strictly valid only for stationary or uniformly moving cylindrical fluid bodies. The analysis given here is certainly inaccurate if significant frictional and form drag occurs at the interface. Such effects would result in non-uniform velocity patterns for the base flow and in important non-linear inertial contributions. Still, the present study provides a basis from which further studies of even these more complex problems can proceed.

Acknowledgement—The authors wish to acknowledge the assistance of Mr. K. L. Yu in carrying out various numerical calculations associated with defining the criteria and bounds for the limiting case solutions.

NOMENCLATURE

- a diameter of an undisturbed cylindrical thread, m
- f functions defined in [20]
- g functions defined in [23]
- i $\sqrt{-1}$
- k wavenumber, m^{-1}
- l parameter defined in [4]
- m parameter defined in [5]
- n parameter defined in [3]
- p hydrostatic pressure, Pa
- q a dummy number (used for the order of Bessel functions)
- r radial coordinate
- t time, s
- u radial component of \mathbf{v}
- \mathbf{v} velocity vector
- w axial component of \mathbf{v}
- x argument in Bessel functions
- z axial coordinate
- C arbitrary constants in [3]–[5]
- D operator defined in [2]
- F functions defined in [10]
- \mathcal{F} functions defined in [11] and listed in the Appendix
- G density ratio ($=\rho_D/\rho_C$)
- $I_q(x), K_q(x)$ modified Bessel Functions of order q with argument x
- M functions defined in [14]
- Oh Ohnesorge numbers ($=(a\sigma\rho)^{1/2}/\eta$)
- P total stress (P_{rz} for shear, P_{rr} for normal stress), Pa
- R_1, R_2 principal radii of curvature, m
- $\text{Re}(\)$ the real part of ()
- S dimensionless growth rate ($=\alpha\theta$)
- U viscosity ratio ($=\eta_D/\eta_C$)
- X wavenumbers, defined in [10]
- X_D, X_C modified wavenumbers, defined in [10]

Greek letters

- α dimensional growth rate, s^{-1}
- β a dummy variable
- Δ difference between two quantities

- ∇ gradient operator, defined in [1]
 η viscosity, Pa · s
 θ characteristic time (defined in table 1), s
 λ wavelength of a disturbance, m
 ν kinematic viscosity ($=\eta/\rho$), m²/s
 π dimensionless numbers, defined in [10]
 ρ density, kg/m³
 σ interfacial tension, Pa · m
 ϕ polar coordinate in cylindrical coordinate system
 ψ stream function, m²/s

Superscripts

- a function of special arguments
 ', " derivatives of the function with respect to its argument
 * the value of this parameter at the maximum growth rate

Subscripts

- C a quantity of the continuous phase
 D a quantity of the dispersed phase
 I a quantity relating to the inertial effects
 V a quantity relating to the viscous effects

REFERENCES

- CHRISTIANSEN, R. M. 1955 The influence of interfacial tension on the breakup of a liquid into liquid jet. Ph.D. Dissertation, Univ. of Pennsylvania, Philadelphia, Pennsylv.
- CHRISTIANSEN, R. M. & HIXSON, A. N. 1957 Breakup of a liquid jet in a denser liquid. *Ind. Engng Chem.* **49**, 1017–1024.
- GOREN, S. L. 1962 The instability of an annular thread of fluid. *J. Fluid Mech.* **12**, 309–319.
- GOREN, S. L. 1964 The shape of a thread of liquid undergoing break-up. *J. Colloid Sci.* **19**, 81–86.
- GRANT, R. P. & MIDDLEMAN, S. 1966 Newtonian jet stability. *AIChE J.* **12**, 669–678.
- KARAM, H. J. & BELLINGER, J. C. 1968 Deformation and breakup of liquid droplets in a simple shear field. *I & EC Fund.* **7**, 576–581.
- LEE, W. K. 1972 Deformation and breakup of liquid drops and threads in extensional flow fields. Ph.D. Dissertation, Univ. of Houston, Houston, Texas.
- MIESSE, C. C. 1955 Correlation of experimental data on the disintegration of liquid jets. *Ind. Engng Chem.* **47**, 1690–1701.
- MEISTER, B. J. & SCHEELE, G. F. 1967 Generalized solution of the Tomotika stability analysis for a cylindrical jet. *AIChE J.* **13**, 682–688.
- VON OHNESORGE, W. 1936 Die bildung von tropfen an düssen und die auflösung flüssiger strahlen. *ZAMM* **16**, 355–358.
- PONSTEIN, J. 1959 Instability for rotating cylindrical jets. *Appl. Sci. Res.* **A8**, 425–456.
- PLATEAU, M. 1873 *Statique des Liquides*. Gauthier–Villars, Paris.
- RAYLEIGH, LORD 1878 On the instability of jets. *Proc. Lond. Math. Soc.* **10**, 4–13.
- RAYLEIGH, LORD 1879 On the capillary phenomena of jets. *Proc. R. Soc. Lond.* **29**, 71–97.
- RAYLEIGH, LORD 1892a On the instability of a cylinder of viscous liquid under capillary force. *Phil. Mag.* **34**, 145–154.
- RAYLEIGH, LORD 1892b On the instability of cylindrical fluid surfaces. *Phil. Mag.* **34**, 177–180.
- TAYLOR, G. I. 1934 The formation of emulsions in definable fields of flow. *Proc. R. Soc. Lond.* **A146**, 501–523.
- TOMOTIKA, S. 1935 On the instability of a cylindrical thread of a viscous liquid surrounded by another viscous fluid. *Proc. R. Soc. Lond.* **A150**, 322–337.

WEBER, C. 1931 Zum zerfall eines flüssigkeitsstrahles. *ZAMM* 11, 136–154.

WHITAKER, S. 1976 Studies of the drop-weight method for surfactant solutions—III. Drop stability, the effect of surfactants on the stability of a column of a liquid. *J. Coll. Interface Sci.* 54, 231–248.

YU, K. L. 1974 The deformation and breakup of liquid drops in an extensional flow field, and the instability of stationary and extending liquid threads. M. S. Thesis, Univ. of Houston.

APPENDIX

The quantities \mathcal{F}_1 , \mathcal{F}_2 , \mathcal{F}_3 and \mathcal{F}_4 in [11] are of the following forms:

$$\mathcal{F}_1 = \left[U \left\{ (X_D^2 + X^2) \left[X \frac{K_0}{K_1} - X_C \frac{\bar{K}_0}{\bar{K}_1} \right] \right\} + \left\{ (X^2 - X_C^2) \left[X_C \frac{\bar{K}_0}{\bar{K}_1} + X_D \frac{\bar{I}_0}{\bar{I}_1} \right] \right. \right. \\ \left. \left. + (X^2 + X_C^2) \left[X_C \frac{\bar{K}_0}{\bar{K}_1} - X \frac{K_0}{K_1} \right] \right\} \right] \left(\frac{I_0}{I_1} \right),$$

$$\mathcal{F}_2 = \left[U \left\{ (X_D^2 + X^2) \left[X_D \frac{\bar{I}_0}{\bar{I}_1} - X \frac{I_0}{I_1} \right] + (X^2 - X_D^2) \left[X_C \frac{\bar{K}_0}{\bar{K}_1} + X_D \frac{\bar{I}_0}{\bar{I}_1} \right] \right\} \right. \\ \left. + \left\{ (X^2 + X_C^2) \left[X \frac{I_0}{I_1} - X_D \frac{\bar{I}_0}{\bar{I}_1} \right] \right\} \right] \left(\frac{K_0}{K_1} \right),$$

$$\mathcal{F}_3 = U \left\{ \left[X_C \frac{\bar{K}_0}{\bar{K}_1} - X \frac{K_0}{K_1} \right] \left((X^2 + X_D^2) \left[X_D \frac{\bar{I}_0}{\bar{I}_1} - X \frac{I_0}{I_1} \right] + (X^2 - X_D^2) \left[X_D \frac{\bar{I}_0}{\bar{I}_1} - 1 \right] \right) \right\} \\ + \left\{ \left[X \frac{I_0}{I_1} - X_D \frac{\bar{I}_0}{\bar{I}_1} \right] \left((X^2 + X_C^2) \left[X_C \frac{\bar{K}_0}{\bar{K}_1} - X \frac{K_0}{K_1} \right] + (X^2 - X_C^2) \left[X_C \frac{\bar{K}_0}{\bar{K}_1} + 1 \right] \right) \right\},$$

and

$$\mathcal{F}_4 = U \left\{ (X^2 - X_D^2) \left[X \frac{K_0}{K_1} - X_C \frac{\bar{K}_0}{\bar{K}_1} \right] \right\} + \left\{ (X^2 - X_C^2) \left[X \frac{I_0}{I_1} - X_D \frac{\bar{I}_0}{\bar{I}_1} \right] \right\}.$$